

# Effective reflectivity and heat generation in sucrose and PMMA mixtures

Maria Paz Gutierrez<sup>a,\*</sup>, Tarek I. Zohdi<sup>b,1</sup>

<sup>a</sup> Department of Architecture, University of California, Berkeley, United States

<sup>b</sup> Department of Mechanical Engineering, University of California, Berkeley, United States



## ARTICLE INFO

### Article history:

Received 24 May 2013

Received in revised form 11 October 2013

Accepted 14 November 2013

### Keywords:

Sucrose

PMMA mixture

Reflectivity

Heat generation

Thermal mass

## ABSTRACT

Recent efforts in the construction sector to develop panels made of agricultural waste and polymer mixtures are becoming more frequent. These panels are usually developed in pursuit of low embodied energy, biodegradability and energy efficiency. PMMA's transparency and structural advantages over other thermoplastics is making this material progressively more common in façades. While advances in PMMA's recyclability are under development, the process still presents multiple challenges regarding environmental efficiency and resulting structural integrity. It is important, therefore, to establish mixtures where PMMA's structural advantages are balanced with low carbon emission substrates, such as agricultural wastes. Typically, agricultural waste in architectural panels is used for structural reinforcement (i.e. fibers). However, agro-derived materials such as sucrose have additional and/or alternative potentials in construction applications. Sucrose's unique optical properties can be implemented for light and thermal control. Additionally, since the energy losses of buildings concentrate in the envelopes another major challenge of cladding substrates pertains to how the façade material can improve energy efficiency, i.e. acting as thermal mass while providing light transmission control avoiding conditions such as glare. Façade materials that can minimize environmental impact while supporting energy savings and appropriate natural light conditions bear strong potential for advancing sustainable building technologies. This analysis provides an expression for the overall reflectivity of combinations of sucrose and PMMA, as well as, estimates of the thermal heating rate, as a function of the relative volume fractions and material properties.

© 2013 Elsevier B.V. All rights reserved.

## 1. Introduction

### 1.1. PMMA properties and building enclosures

From MIT/Monsanto's *House of the Future* (1957) to Matti Suuronen's *Futuro* (1968), the earliest investigations of polymers in the building industry primarily took a single-solution perspective, where polymers were used in every component possible [1, pp. 8–24]. Since the 1970s, however, the increasing cost of petroleum as well as an awareness of the environmental impact of polymers led to a reevaluation of their use in buildings. The enormously wide variety of properties and available characteristics led to a leveraging

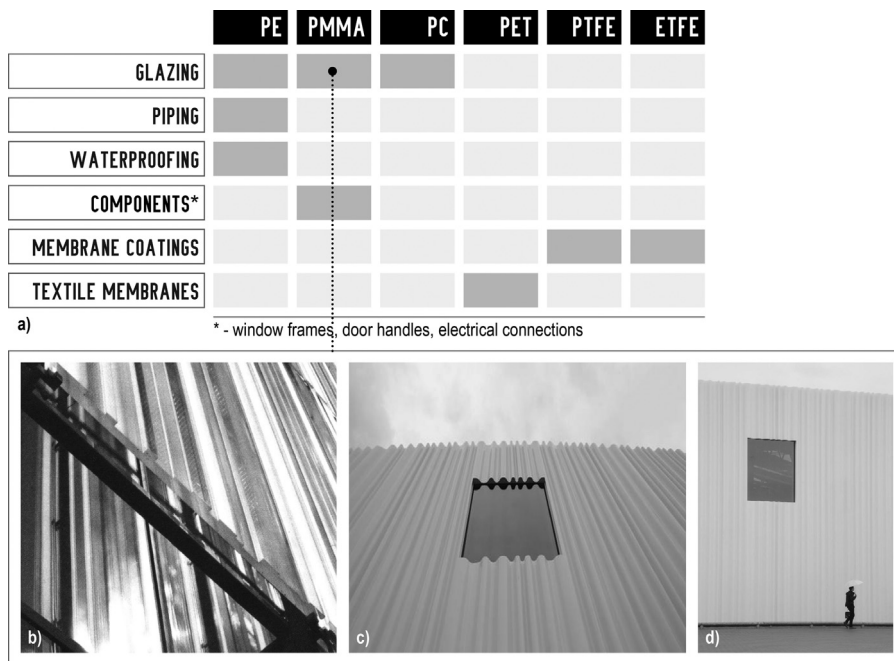
of the strengths of individual polymers whose use became tailored for very specialized applications [2, pp. 10–16]. These uses range from vapor barriers, protective coverings, paints, and insulation (Fig. 1A) applications. Amongst the most used thermoplastics in these applications are polyethylene (PE), polyvinyl chlorine (PVC), and polystyrene (PS).

In the last decade, we have seen a rising interest in increasing the use of thermoplastics as building enclosures as films, surface cladding, and structural modules. From a more frequent use of PC to EFT, buildings with thermoplastics exteriors are becoming increasingly ubiquitous. The desire to work with substrates of comparative transparency to glass that can also be easily fabricated through digital processes for variable formal and esthetic effects in building façades is taking architects to experiment with thermoplastics traditionally not used for exterior applications. With this purpose, architects are turning toward implementing PMMA onto façades due to the material's optic and mechanical properties, as well as, easy forming and surfacing characteristics (Fig. 1B). Acrylic façades currently clad large buildings in applications that reach over 500 m length (Fig. 1C).

\* Corresponding author at: Department of Architecture, University of California, Berkeley, 353 Wurster Hall, Berkeley, CA 94720-1820, United States.  
Tel.: +1 510 642 4942.

E-mail addresses: [mpazgut@berkeley.edu](mailto:mpazgut@berkeley.edu), [mpazgut@hotmail.com](mailto:mpazgut@hotmail.com)  
(M.P. Gutierrez), [zohdi@me.berkeley.edu](mailto:zohdi@me.berkeley.edu) (T.I. Zohdi).

<sup>1</sup> Address: Department of Mechanical Engineering, University of California, Berkeley, 6117 Etcheverry Hall, Berkeley, CA 94720-1740, United States.  
Tel.: +1 510 642 9172.



The physical properties of PMMA give it a distinct advantage in selection over other thermoplastics currently used in exterior applications in buildings. One of its chief advantages is its relatively high weathering resistance (Fig. 2A). PC, often characterized as comparable to PMMA (mechanical and optic properties) for construction applications, does not weather well. PC typically requires additives to prevent yellowing through time. ETFE, a progressively common material in high-performance buildings enclosures, on the other hand weathers extremely well and is advantageous as thermal barrier [3]. Nevertheless, ETFE's thermal performance is still arguable regarding typical glass and its

structural properties render the material more suitable for thin membrane applications (often air compression-based) rather than as structural panels [4, pp. 486–495, 5]. It is important to note that the mechanical properties of thermoplastics tend to be highly dependent on temperature and have a relatively narrow service temperature range. PMMA, for example, has a coefficient of thermal expansion nearly seven times that of steel. While it has the undesirable characteristic of a brittle failure mode, PMMA has a high enough upper stress limit that renders it suitable for façade (panel) applications [2, pp. 225–285]. By contrast, the ductile PC and PE deform plastically under low stress (Fig. 2B).

	DENSITY [g/cm <sup>3</sup> ]	SERVICE TEMP. LONG / SHORT [°C]	TENSILE STRENGTH [N/mm <sup>2</sup> ]	ELASTIC MODULUS [N/mm <sup>2</sup> ]	COEFF. OF LINEAR THERMAL EXPANSION [10 <sup>-4</sup> /K]	THERMAL CONDUCTIVITY [W/mK]	RESISTANCE TO CHEMICAL ATTACK FROM:
PE LD	0.92	60-75/80-90	8-23	200-500	230-250	0.32-0.40	acids      alkalis      weather
PE HD	0.95	75-90/90-120	18-35	700-1400	120-200	0.38-0.51	● ● ● ●      ● ● ● ● ●      ○
PMMA	1.19	65-90/85-100	50-77	1600-3600	70-90	0.18	○ ○      ● ● ● ●      ● ● ● ● ●
PC	1.20	135/160	56-67	2100-2400	60-70	0.21	○ ○      ○ ○ ○ ○      ○ ○
PET	1.37	100/200	47	3100	40-60	0.24	○ ○ ○      ○ ○ ○ ○      ○ ○
PTFE	2.17	250/300	25-36	410	120-250	0.25	● ● ● ●      ● ● ● ● ●      ● ● ● ● ●
ETFE	1.75	150/220	35-54	1100	40	0.23	● ● ● ●      ● ● ● ●      ● ● ● ●

**Fig. 2.** Properties of thermoplastics used in exterior building applications diagram by author from [2].

## 1.2. Environmental and cost potential of PMMA and agricultural waste mixtures

While PMMA offers multiple mechanical and weathering advantages when compared to other thermoplastics currently used in building enclosures it is a material that as most synthetic polymers requires high energy for manufacturing and have strong long terms environmental impacts. Literature has discussed largely this topic in life cycle analysis research [6, pp. 3436–3445]. In response to a growing awareness toward environmentally sensitive construction materials, research in bioplastics and natural waste-synthetic polymer mixtures has been growing particularly since the past decade [7, pp. 19–26]. A significant field of research in biodegradable polymers pertains to the incorporation of agriculturally derived particles [8, pp. 822–825]. These mixtures offer various sustainable advantages including biodegradability.

PMMA based mixtures are common to many industrial applications (see <http://www.marketsandmarkets.com/Market-Reports/polymethyl-methacrylate-pmma-market-715.html>). In fact, this compound has a higher blending compatibility with other thermoplastics when compared to most common typical façade substrates (PC, PE, PET) (Fig. 3). The broad range of compatibility of PMMA with various naturally derived fillers, i.e. plant fibers, has led to expansive experimentation for construction applications. However, these have concentrated fundamentally on interior finishes uses. The experimentation of naturally derived particles or fibers into PMMA matrices for exterior building applications remains largely unexplored. Nevertheless, this frontier can yield significant advantages that range from weight to cost.

Advancements in PMMA and naturally derived particles mixtures can also be highly beneficial from an environmental standpoint. Significant progress has occurred in plastic recyclability particularly in the last decade [9]. However, PMMA recycling still presents some crucial challenges. For one part, PMMA cannot be easily recycled to monomer by simple chemical methods unlike condensation polymers as PET [10, pp. 2564–2575]. The required processes for depolymerization of PMMA, including that the raw condensate of PMMA, may result in contamination by the metal used or other byproducts of the recycling procedure. Research points toward advances in the preservation of mechanical properties after the recycling of thermoplastics. Tensile strain at break in PMMA and mixtures with this material [9] remains an exception to this progress. While to some industries this may not be a relevant factor in a façade application, tensile strain weaknesses are important for decrease in structural stability [2, pp. 134–150, 11, pp. 90–119].

### 1.2.1. Agricultural waste: sucrose potential for construction

Literature has discussed extensively in the recent years the potential advantages of incorporating agriculturally derived materials including waste in construction. For most part researchers have focused in evaluating the structural advantages of materials such as flax, hemp, rice husks, sugar cane bagasse, in concrete [12,13]. In few cases, the structural advantages have also been co-evaluated with thermal conductivity [14]. However, other significant innovation fronts from agro-based materials in construction (i.e. optical) remain largely unexplored. Sucrose distinguishes itself in this front due to its highly unique optical properties with a refractive index of equivalent ranges (1.4–1.55) to clear glass or PMMA [15]. The use of agricultural waste in construction panels for optical control has strong promise for various architectural applications. A key component of human comfort pertains to balancing daylight transmission to interior spaces without excess heat and preventing glare.

Glare is defined as the excessive luminance and/or excessive luminance ratios in the field of vision, fundamental in the determination of visual comfort that must be prevented in daylit spaces. On the other hand, visual comfort on a work plane depends on both the illuminance level and its distribution. These can be either direct or discomfort glare, and reflected glare or veiling glare [16]. If the light source is in the field of vision, we refer to it as direct glare. Conversely, if caused by the reflection of a light source on a surface, literature refers to the phenomenon as reflected glare. Current building standards and codes require indoor illuminance levels on the working plane, which vary widely among countries and depend on the activity levels [17]. Several luminescence recommendation ranges for tasks exist. Depending on the types of buildings and rooms, these ranges span from 200 to 2000(lux) [38]. Literature estimates ~50 foot candles on the working face plane for appropriate light comfort levels [17]. In parallel, glazing incorporates through multiple advances in building technologies and simulation, which span from films to electrochromic windows, new methods to control reflectivity effectively [18]. Intensive research in this frontier points toward the need to improving daylight strategies and daylight availability metrics in buildings [19].

While large fenestrations provide good amounts of light and pleasant outdoor views they also contribute significantly to heat gains and/or losses, as well as, potential glare. Advances in transparent conductors with spectral selectivity, angular selectivity, and temporal chromatic variability, as well as double and triple glazing have been widely discussed in literature [20–26]. IGDB (<http://windowoptics.lbl.gov/data/igdb/igdb>) provides an extensive optical data update for glazing (monolithic, laminate, applied films, and coating) products. These products present a wide array of variations ranging from extremely low solar reflectance i.e. clear float glass (0.077 front and back-3 mm Optiglass) or commercial PMMA (0.07 front and back-3 mm Atofina) to coated glazing (0.438-front/0.535-back, ClimaGuard-on 3 mm clear glass). Fig. 4 presents a sampling of current products in each category (monolithic, laminate, coating, and film) indexing the wide surface variability from ~90% to 10% light absorption. The aforementioned literature discusses the integration of efficient reflectivity and thermal conductivity through various coating films technologies, double and triple glazing systems. Mohelnikova [23] study presents new glazing technologies with IR reflective thin film (45 nm TiO<sub>2</sub>–25 nm Ag–45 nm TiO<sub>2</sub>) with reflectivity ~0.3 used for effective reflectance and thermal control. Glazing systems currently have a heat transfer coefficient of ~1 W/m<sup>2</sup> K. However, values of as ~0.2 W/m<sup>2</sup> K may be possible by combining vacuum insulation with low-emittance-coated glass enabling a reduction of 80% of thermal conductivity [26].

More recently, researchers are developing models which address the large impact in heat transfer of long wave radiation [heat exchange] between inside and outside surfaces through glazing [27]. Wang et al. model defines that when the long radiation transmittance of glass reaches 0.1 the effect of long-wave transparency radiation is substantial. This is comparable to the spectral radiation of low-e glazing ~0.1 [23]. Advances in this area are important to typical transparent glass and a broad array of polymeric glazing including PMMA [27].

In Table 1, we see a projection of the potential of a PMMA–sucrose mixture regarding material cost, embodied energy and carbon emission for a panel of a standard enclosure size of: 3' × 6' × 1/4". We have chosen to compare the PMMA–sucrose mixture with transparent glass, pure PMMA, PC, PE, and PMMA–bamboo mixture. The choice to evaluate a bamboo mixture stems from the fact that this substance is recognized as the plant with probably the lowest embodied energy and carbon emission in construction. Bamboo's

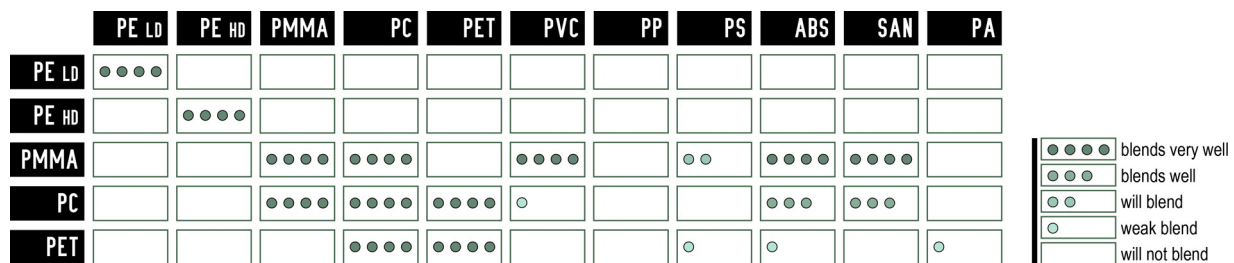


**Fig. 3.** PMMA blending capacities with polymers typically used in industry, diagram by author from Knippers et al. [2] and Rybnicek et al. [9].

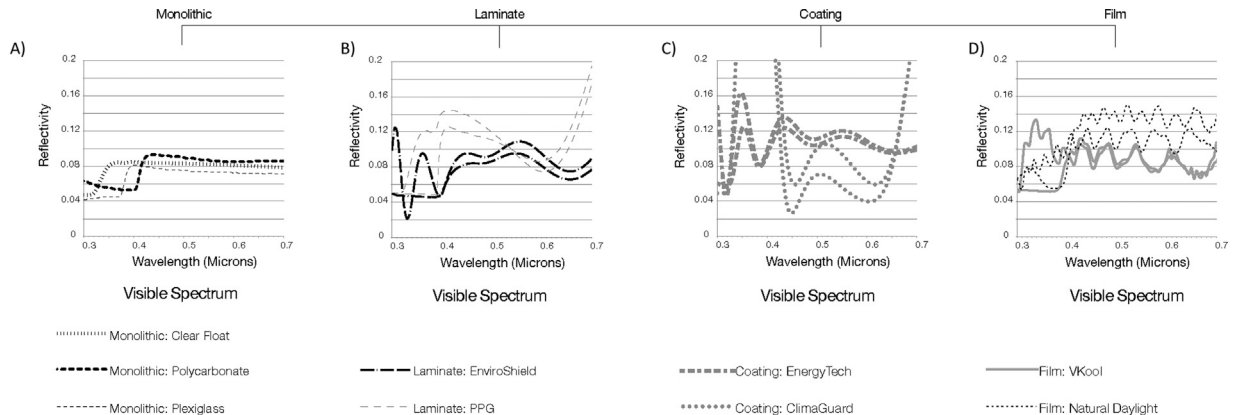


**Fig. 4.** (A) Comparison of front surface reflectance of glazing types; (B) Comparison of back surface reflectance of glazing types; (C) Comparison of back and front surface reflectance of glazing types, diagram by author plotted from IGDB data (<http://windowoptics.lbl.gov/data/igdb/igdb>).

footprint is lower than hemp or flax, which are widely acknowledged as extremely low carbon footprints materials in construction (<http://www.eurostar-ep.com/en-us/news/12-149/carbonfootprint.aspx>).

The PMMA-sucrose mixture panel (60% sucrose) has the potential of a material cost of approximately 25% of the cost of glass and 40% of the cost of a PMMA panel. In addition, the PMMA-sucrose mixture panel (60% sucrose) would cost approximately 25% of the cost of a PMMA and bamboo particle (60% bamboo) mixture. From an environmental perspective, the PMMA-sucrose mixture (60% sucrose) panel has the potential of being 24% of the total embodied energy of glass and 40% of a PMMA panel. Since bamboo has the lowest carbon emission of all construction materials the fact that

the PMMA-sucrose mixture at 60% sucrose concentration is three times higher and of equal low embodied energy is advantageous. This is particularly the case if we consider that the mixture uses low-grade sucrose crystals, costs only a quarter fraction, and has the potential significant energy savings derived from thermal mass and optical properties for effective reflectivity.

### 1.3. Thermal storage and reflectivity potential of PMMA and sucrose mixture

In Table 2 we see that a PMMA panel has a significantly lower thermal conductivity (0.18 W/mK) than a typical transparent glass (0.8 W/mK) or in comparison to typical thermoplastics used in

**Table 1**  
Sucrose–PMMA mixture comparative projections (cost/panel, weight, embodied energy) with typical thermoplastics for building enclosures and PMMA mixtures. Projections (cost/panel, weight, embodied energy) for sucrose–PMMA mixture in comparison to transparent glass, translucent glass, PC, PE, PMMA, PMMA with bamboo sheets, PMMA with sucrose mixture [12–17].<sup>a</sup>

	Cost	Cost/ft <sup>2</sup>	Density (g/cm <sup>3</sup> )	Panel size	Embodied Energy	GWP (kg CO <sub>2</sub> /kg)
Transparent glass <sup>a</sup>	\$180.00	\$10.00	2.5	3' × 6' × 0.25"	349.65	21.8
PC	\$193.71	\$10.76	1.2	3' × 6' × 0.25"	78.92	11.66
PE	\$143.81	\$7.99	0.92	3' × 6' × 0.25"	87.1	3
PMMA	\$115.00	\$6.40	1.19	3' × 6' × 0.25"	207.3	14.7
Bamboo	\$230.00	\$12.80	0.95	3' × 6' × 0.25"	0.015 <sup>b</sup>	0.2
Sucrose	\$1.08	\$0.06	1.55	3' × 6' × 0.25"	0.037 <sup>c</sup>	31
40% PMMA/60% bamboo	\$184.00	\$10.24	1.046	3' × 6' × 0.25"	82.80 <sup>d</sup>	6
40% PMMA/60% sucrose	\$46.65	\$2.62	1.35	3' × 6' × 0.25"	82.94 <sup>e</sup>	24.48

Frames vary substantially and so are not included in the weight for this comparison.

<sup>a</sup> AGC – Planibel glass, 8 mm, mid-high end glass from one of the largest glass manufacturers worldwide.

<sup>b</sup> Estimate of embodied energy based on organic component (100% bamboo pulp).

<sup>c</sup> Estimate of embodied energy based on organic component (100% sucrose).

<sup>d</sup> Estimate of embodied energy based on organic component of panel at 60% bamboo particles.

<sup>e</sup> Estimate of embodied energy based on organic component of panel at 60% sucrose concentration.

<sup>f</sup> See [http://www.marketsandmarkets.com/Market-Reports/poly\(methyl-methacrylate\)-pmma-market-715.html](http://www.marketsandmarkets.com/Market-Reports/poly(methyl-methacrylate)-pmma-market-715.html), <http://www.indexmundi.com/commodities/?commodity=sugar>, <http://comtrade.un.org/db/ce/ceSnapshot.aspx?px=H3&cc=441210>, <http://www.eurostar-ep.com/en-us/news/12-149/carbonfootprint.aspx> and <http://www.interplastic.com>.

**Table 2**

PMMA–sucrose mixture comparative projections (thermal conductivity, reflectivity) with typical thermoplastics for building enclosures and PMMA mixtures, and transparent glass. Comparative projection of PMMA–sucrose mixture panel (thermal conductivity, reflectivity) in relation to transparent glass, PMMA, PC, PET [2].

#### Thermal and optical properties

	Thermal conductivity (W/m K)	Reflectivity	Transmissivity	Refractive index <sup>d</sup>
Transparent glass <sup>a</sup>	0.8–1.0	0.08	0.87	1.52
PC <sup>b</sup>	0.32–0.40	0.09	0.76	1.585
PE (film)	0.42–0.51	0.09	0.05 <sup>e</sup>	1.575
PMMA <sup>b</sup>	0.18	0.07	0.8	1.489
PMMA with bamboo	0.031			

<sup>a</sup> AGC – Planibel glass, 8 mm, mid-high end glass from one of the largest glass manufacturers worldwide.

<sup>b</sup>  $t = 8$  mm.

<sup>c</sup>  $t = 3$  mm.

<sup>d</sup> At standard sodium doublet  $\lambda = 589$  nm.

<sup>e</sup> Very low transmissivity at UV and visible spectrums.

building enclosures, i.e. PC (0.35 W/mK) and PE (0.45 W/mK) correspondingly. For internal climatic comfort and energy savings, the thermal conductivity of architectural enclosures is crucial. As aforementioned, building envelopes is the zone where energy losses are concentrated [28,29]. Thermal mass is pivotal for energy efficiency in buildings envelopes for various climate zones [30, pp. 763–773]. Moreover, climate regions that benefit from thermal mass often require decrease in transparency for internal spaces due to glare produced by direct light [31, pp. 139–145]. In Table 2, we also see that PMMA has a refractive index comparative or higher than clear glass ranging typically from 1.4 to 1.55 [32,33]. As aforementioned, sucrose also typically fits within a comparative refractive index of 1.4–1.5 [15] similar to clear glass and PMMA.

In an attempt to provide thermal insulation and daylight transmission control in building enclosures, architects, engineers, and scientists are researching systems that can be translucent and efficient insulators, such as, PC with aerogel granules [34]. Hence, a panel system that can provide the weight, cost, and environmental advantages of a PMMA–sucrose substrate projected in Table 1 and function as a thermal mass with effective reflectivity has strong overall potential for future energy efficient enclosures.

This paper evaluates synchronously the thermal storage and effective reflectivity potential of PMMA and sucrose mixtures for a future building material panel (Fig. 5). This study is set to narrow the range of experiments (i.e. structural and weathering resistance) required to evaluate this mixture's potential for future façade applications.

## 2. Theory and calculation

Consider a beam of light incident upon a boundary separating two different materials, which produces a reflected wave and a transmitted (refracted/absorbed) wave (Fig. 5). The amount of incident electromagnetic energy ( $I_i$ ) that is reflected ( $I_r$ ) is given by the total reflectance  $R \stackrel{\text{def}}{=} I_r/I_i$  where  $0 \leq R \leq 1$ , where  $R$  is given by Eq. (1.1) for unpolarized electromagnetic radiation, where  $\hat{n}$  is the ratio of the refractive indices of the ambient (incident) medium ( $n_i$ ) and transmitted (absorbing) medium ( $n_t$ ),  $\hat{n} = n_t/n_i$  (see Gross et al. [35] for example)

$$R = \frac{I_r}{I_i} = \frac{1}{2} \left( \left( \frac{(\hat{n}^2/\hat{\mu}) \cos \theta_i + (\hat{n}^2 - \sin^2 \theta_i)^{1/2}}{(\hat{n}^2/\hat{\mu}) \cos \theta_i + (\hat{n}^2 - \sin^2 \theta_i)^{1/2}} \right)^2 + \left( \frac{\cos \theta_i + (1/\hat{\mu})(\hat{n}^2 - \sin^2 \theta_i)^{1/2}}{\cos \theta_i + (1/\hat{\mu})(\hat{n}^2 - \sin^2 \theta_i)^{1/2}} \right)^2 \right), \quad (1.1)$$

where the refractive index is defined as the ratio of the speed of light in a vacuum ( $c$ ) to that of the medium ( $v$ ), where  $c = 1/\sqrt{\epsilon_0 \mu_0} \approx$

$2.99792458 \times 10^8 \pm 1.1$  m/s,  $v = 1/\sqrt{\epsilon \mu}$ , ( $\epsilon$ ) is the electric permittivity and ( $\mu$ ) is the magnetic permeability.<sup>2</sup> In Eq. (1.1),  $\hat{\mu}$  is the ratio of the magnetic permeabilities of the surrounding incident medium ( $\mu_i$ ), and transmitted (absorbing) medium ( $\mu_t$ ),  $\hat{\mu} = \mu_t/\mu_i$ . We consider application where the magnetic permeability is, within experimental measurements, virtually the same for both the matrix and particle phases. Thus, for the remainder of the work, we shall take  $\hat{\mu} = 1$  ( $\mu_0 = \mu_i = \mu_t$ ) and, thus,  $\hat{n} = (n_t/n_i) = \sqrt{\epsilon_t \mu_t / \epsilon_i \mu_i} \Rightarrow \epsilon_t \mu_t = (\hat{n})^2 \epsilon_i \mu_i \Rightarrow \epsilon_t = (\hat{n})^2 \epsilon_i$ , where  $\epsilon_i = \epsilon_0$  (vacuum permittivity). Notice that as  $n \rightarrow 1$  we have complete absorption, while as  $n \rightarrow \infty$  we have complete reflection. The total amount of absorbed power by the material is  $(1-R)I_i$ . The angle between the point of contact of a beam (Fig. 5) and the outward normal to the surface at that point is the angle of incidence ( $\theta_i$ ).

The classical reflection law states that the angle at which a beam is reflected is the same as the angle of incidence and that the incoming (incident,  $\theta_i$ ) and outgoing (reflected,  $\theta_r$ ) beam lays in the same plane, and  $\theta_i = \theta_r$ . Furthermore, refraction law states that, if the beam passes from one medium into a second one (with a different index of refraction), and if the index of refraction of the second medium is less than that of the first, the angle the ray makes with the normal to the interface  $n \stackrel{\text{def}}{=} (c/v) = \sqrt{\epsilon \mu / \epsilon_0 \mu_0} = (\sin \theta_i / \sin \theta_t)$ ,  $\theta_t$  being the angle of the transmitted ray (Fig. 5),  $c$  is the propagation speed in the incident medium. Specifically, if the beam is directly incident ( $\theta_i = 0$ )

$$R = \frac{I_r}{I_i} = \left( \frac{\hat{n} - \hat{\mu}}{\hat{n} + \hat{\mu}} \right)^2 = \left( \frac{\sqrt{\epsilon_t/\epsilon_i} - \sqrt{\mu_t/\mu_i}}{\sqrt{\epsilon_t/\epsilon_i} + \sqrt{\mu_t/\mu_i}} \right)^2 = \left( \frac{\sqrt{\hat{\epsilon}} - \sqrt{\hat{\mu}}}{\sqrt{\hat{\epsilon}} + \sqrt{\hat{\mu}}} \right)^2 \quad (1.2)$$

For more details see the cited literature [35–39, pp. 3125–3131, 40–42, pp. 256–277, 43, pp. 969–981; 44–46].

### 2.1. Effective reflectivity of mixture

For mixtures of the chosen materials, we use the effective electric permittivity  $\epsilon^*$  and magnetic permeability  $\mu^*$  to construct the effective reflectivity:

$$R^* = \frac{I_r}{I_i} = \left( \frac{\sqrt{\hat{\epsilon}^*} - \sqrt{\hat{\mu}^*}}{\sqrt{\hat{\epsilon}^*} + \sqrt{\hat{\mu}^*}} \right)^2 \quad (2.1)$$

<sup>2</sup> The free space electric permittivity is  $\epsilon_0 = 1/c^2 \mu_0 = 8.8542 \times 10^{-12}$  C N<sup>-1</sup> m<sup>-2</sup> and the free space magnetic permeability is  $\mu_0 = 4\pi \times 10^{-7}$  Wb A<sup>-1</sup> m<sup>-1</sup>.

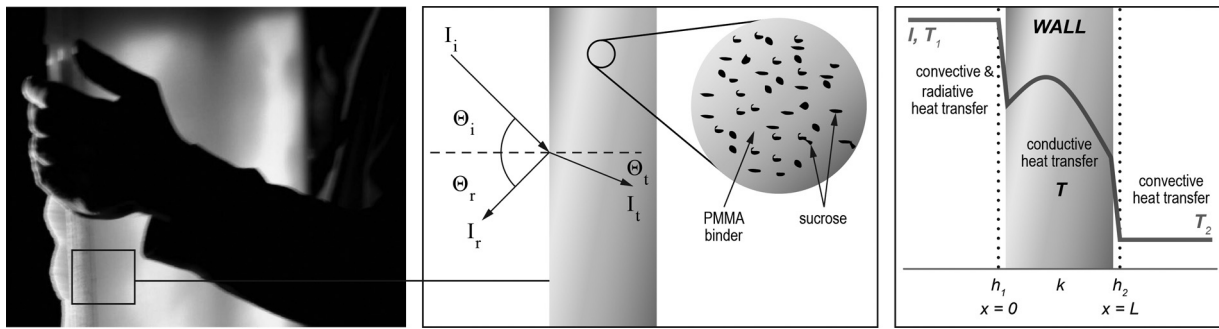


**Fig. 5.** (A) Mixture sucrose PMMA panel prototype; (B) incoming beam of light diagram of PMMA–sucrose mixture; and (C) convective and radiative heat transfer diagram of PMMA–sucrose mixture.

For example, for a two-phase medium, relatively simple upper and lower estimates for the effective electric permittivity and magnetic permeability are the so-called Wiener [42] bounds:

$$\left(\frac{\nu_2}{\epsilon_2} + \frac{1-\nu_2}{\epsilon_1}\right)^{-1} \leq \epsilon^* \leq \nu_2 \epsilon_2 + (1-\nu_2) \epsilon_1 \quad (2.2)$$

where  $\nu_2$  is the volume fraction of the particles (phase 2),  $\epsilon_2$  is the permittivity of the particles,  $\epsilon_1$  is the permittivity of the matrix (phase 1) and

$$\left(\frac{\nu_2}{\mu_2} + \frac{1-\nu_2}{\mu_1}\right)^{-1} \leq \mu^* \leq \nu_2 \mu_2 + (1-\nu_2) \mu_1 \quad (2.3)$$

where  $\mu_2$  is the permeability of the particles and  $\mu_1$  is the permeability of the matrix. Hashin and Shtrikman [39] gave sharper bounds of the electric permittivity and magnetic permeability:

$$\underbrace{\epsilon_1 + \frac{\nu_2}{(1/\epsilon_2 - \epsilon_1) + (1-\nu_2/3\epsilon_1)}}_{\epsilon^{*, -}} \leq \epsilon^* \leq \underbrace{\epsilon_2 + \frac{1-\nu_2}{(1/\epsilon_1 - \epsilon_2) + (\nu_2/3\epsilon_2)}}_{\epsilon^{*, +}} \quad (2.4)$$

and

$$\underbrace{\mu_1 + \frac{\nu_2}{(1/\mu_2 - \mu_1) + (1-\nu_2/3\mu_1)}}_{\mu^{*, -}} \leq \mu^* \leq \underbrace{\mu_2 + \frac{1-\nu_2}{(1/\mu_1 - \mu_2) + (\nu_2/3\mu_2)}}_{\mu^{*, +}} \quad (2.5)$$

Simple approximations for the effective parameters can be determined by taking the average of the bounds:

$$\epsilon^* \approx \frac{1}{2}(\epsilon^{*,+} + \epsilon^{*,-}) \quad (2.6)$$

and

$$\mu^* \approx \frac{1}{2}(\mu^{*,+} + \mu^{*,-}) \quad (2.7)$$

For more details see Zohdi [47].

## 2.2. Heat generation

The amount of heat absorbed by a wall can be approximated from an energy balance where we assume that all of the absorbed energy is converted into heat, ignoring convection and conduction:

$$mC \frac{dT}{dt} = I^{\text{absorbed}} A = (1 - R^*) I_i A, \quad (2.8)$$

where  $A$  is the area of the wall,  $m$  is the mass of the wall mixture,  $C$  is the heat capacity of the wall mixture given by:

$$mC \approx ((\rho C)_1 \nu_1 + (\rho C)_2 \nu_2) V \quad (2.9)$$

where  $V$  is the volume of the wall and  $\rho$  is the density. Solving for the rate of temperature increase yields

$$\frac{dT}{dt} = \frac{(1 - R^*) I_i A}{((\rho C)_1 \nu_1 + (\rho C)_2 \nu_2) V} \quad (2.10)$$

## 2.3. Sucrose–PMMA mixture panel example

Below we provide an example of the heat generation and reflectivity of a wall with typical façade panel characteristics. The selected data is approximated from existing literature [48,49].<sup>3</sup>

- Relative electric permittivity for phase 1 (PMMA binder):  $\epsilon_{1r} = \frac{\epsilon_1}{\epsilon_0} = 2.5$
- Relative electric permittivity for phase 2 (sucrose particles):  $\epsilon_{2r} = \frac{\epsilon_2}{\epsilon_0} = 3.5$
- Relative magnetic permeability for phase 1 (PMMA binder):  $\mu_{1r} = \frac{\mu_1}{\mu_0} = 1.0$
- Relative magnetic permeability for phase 2 (sucrose particles):  $\mu_{2r} = \frac{\mu_2}{\mu_0} = 1.0$
- The density for phase 1 (PMMA binder):  $\rho_1 = 1200 \text{ kg/m}^3$
- The density for phase 2 (sucrose particles):  $\rho_2 = 1150 \text{ kg/m}^3$
- The heat capacity for phase 1 (PMMA binder):  $C_1 = 1466 \text{ W/kg}$
- The heat capacity for phase 2 (sucrose particles):  $C_2 = 1244 \text{ W/kg K}$
- The incident radiation is  $I_i = 1367 \text{ W/m}^2$  (maximum intensity)
- Wall dimensions are  $L \times W \times t = 10 \text{ m} \times 3 \text{ m} \times 0.0254 \text{ m}$

In the case that the magnetic permeabilities are equal, we simply use the common value.

See Fig. 6 for results for  $R^*$  and the normalized effective heating rate, defined as:

$$H^* \stackrel{\text{def}}{=} \frac{(dT/dt)(\nu_2)}{(dT/dt)(\nu_2 = 0)} \quad (3.1)$$

## 3. Results and discussion

The energy for spatial cooling amounts to more than 75% of the electrical peak load in hot climates [50]. Thus, the need to advance thermal conductivity in envelopes is fundamental. To achieve efficient strategies of energy saving and visual comfort researchers must consider multiple aspects of daylighting and lighting control (i.e. daylight factor, illuminance and luminance, and glare index).

<sup>3</sup> See <http://www.rgpballs.com>.

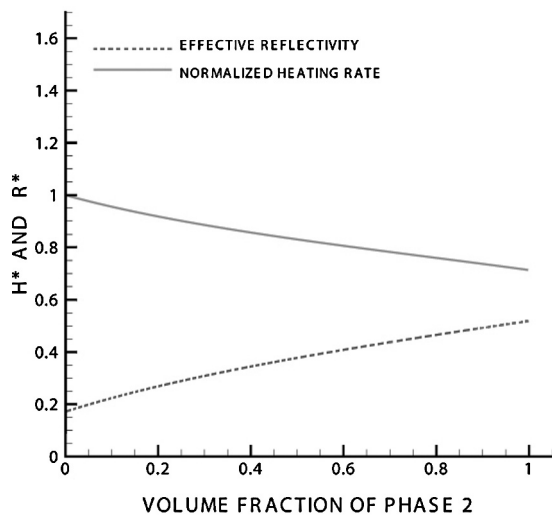


**Fig. 6.** Parameter study for  $R^*$  and  $H^*$  varying the volume fraction of phase 2 (sucrose particles).

Daylighting provides ample benefits for productivity and potential energy savings when combined with artificial lighting systems through lighting control techniques [51]. The primary sources for luminance distribution are the sun, sky, buildings, and ground [52]. Daylighting design must take in consideration latitude, climate, and building orientation, since all these factors affect daylight availability. This term refers specifically to the amount of daylight available from the sun and the sky at a specific location, time, date, and sky condition [52].

New materials and simulation advances evidence the need and awareness to advance glazing systems with integrative thermal and reflectivity advantages including in polymeric substrates. With this basis, we evaluate a material mixture that decreases heat gains while providing efficient reflectivity contributing to glare prevention and potential energy savings. This paper provides simple estimates for the overall reflectivity and the overall heat absorption rate as a function of Sucrose and PMMA properties. The PMMA–sucrose mixture could be used as the material matrix of façade panels in combination with reduced transparent glazing to decrease heat gains and losses and minimize or eradicate glare through effective reflectivity. For our first estimates of reflectivity of the PMMA–sucrose mixture, we assume an incident radiation of  $1367 \text{ W/m}^2$ .

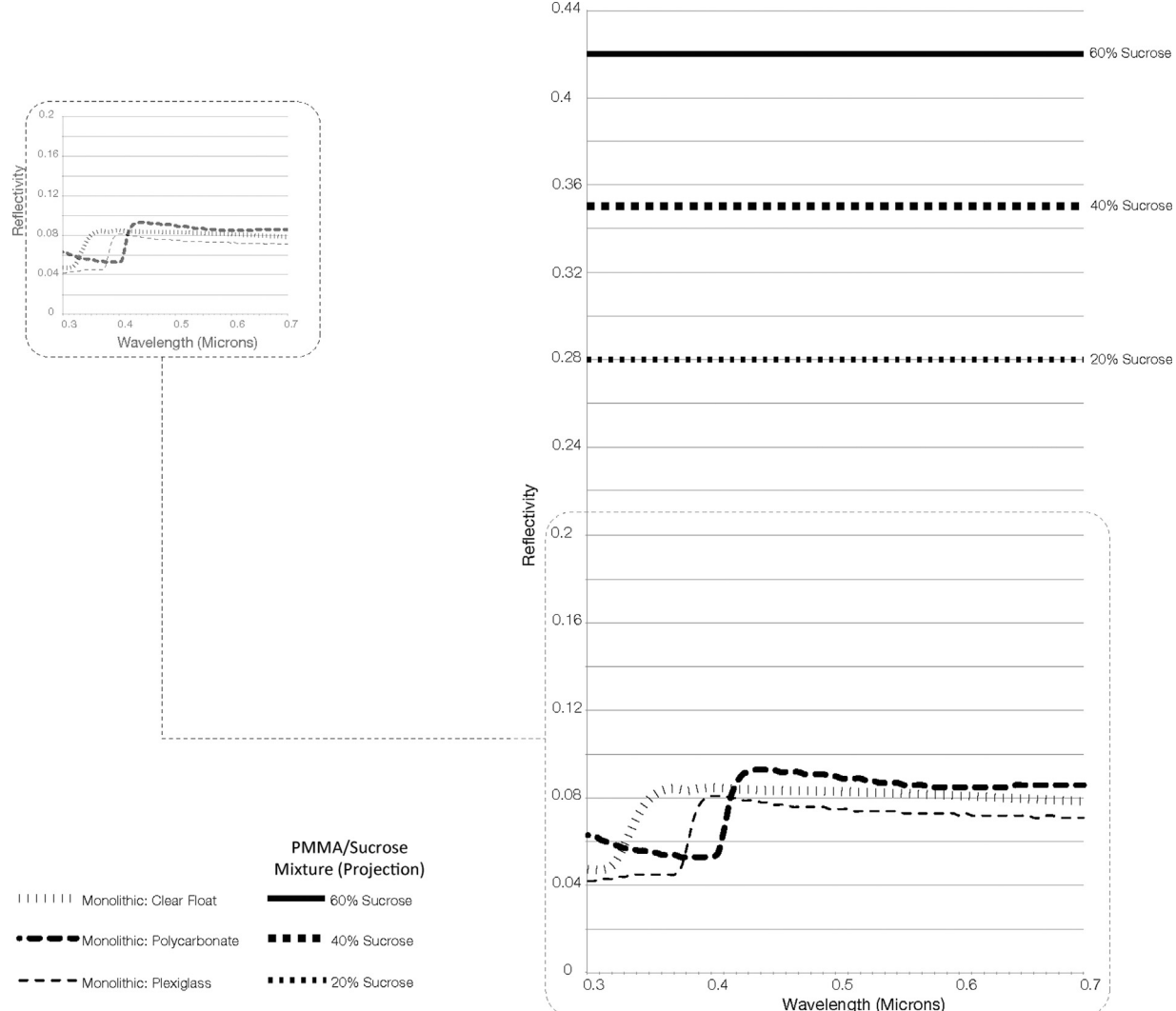


**Fig. 7.** Comparison diagram of reflectivity of monolithic panels (glazing, PMMA, PC, and estimates of PMMA/sucrose mixtures of 20%, 40% and 60% concentration).

An understanding of the combination effect between optical and thermal properties is important to achieve the applicability of the PMMA–sucrose structure. In this simulation, we compared the reflectivity and normalized heating rate as a function of the volumetric fraction of sucrose in the mixture. As seen in Fig. 6, the fraction of sucrose in the wall assembly significantly affects its potential performance as an applied material. Based on the increased reflectivity and absorption as the percentage of sucrose increases, transmission of electromagnetic radiation must decrease. Varying the percentage of sucrose should therefore affect the direct transfer of light and heat.

Fig. 6 presents that the mixture would have an 83% light absorption (Pure PMMA) at 0% sucrose with a decrease to 65% [40% sucrose concentration] and to 45% [80% sucrose concentration] correspondingly. Hence, the effective reflectivity increases around 50% with a concentration of approximately 80% of sucrose.

Fig. 7 shows the relatively high values of reflectance (visible wavelength) for various concentrations of sucrose in the mixture. This allows the mixture to reduce the amount of transmitted light to the interior space without absorbing and reemitting the excess energy. The projections presented in Fig. 7 point a 28% reflectivity for 20% sucrose concentration; 35% reflectivity for 40% sucrose concentration and 42% reflectivity for 60% sucrose concentration for the panels. Commercial PMMA (Plexiglass) of 6 mm averages 8% reflectivity based on IGDB data. Utilizing this strategy allows for relatively high thermal insulation without a reliance on low-E coatings or multiple-pane window systems. For areas that require daylight control this system could be a very cost-effective solution.

The normalized heat rate in Fig. 6 projects a 15% reduction at 20% sucrose concentration. The heating rate reduction at 60% and 80% sucrose concentration is of 20% and 25% correspondingly. At a full concentration of sucrose the table presents a reduction of approximately one third (heating rate) in comparison to pure PMMA. Fig. 6 presents a potential range of optimized reduction between 15% and 20% in heating rate and an effective reflectivity between 65% and 40% at 60% sucrose concentration in comparison to pure PMMA.

The incorporation of substrates as monolithic aerogel is presenting promising results in higher effective reflectivity and thermal reduction of glazing. Buratti and Moretti [53] demonstrated that monolithic aerogel glazing has the best performance with respect to granular aerogel for light transmittance (0.62 between two 4 mm float glasses) and thermal insulation ( $0.6 \text{ W m}^{-2} \text{ K}^{-1}$ ) under a solar factor of 0.74. The study presents that monolithic aerogel between two 4 mm float glasses enabled a 62% reduction in heat losses, and a 17% reduction in light transmittance when compared to a double glazing with a low-e coating [53]. The concentration range between 40% and 60% sucrose appears to be the most promising in the PMMA sucrose mixture, concerning heating decrease potential and effective reflectivity. The next phase of research will focus on this range (40–60% sucrose concentration) to test empirically the heating rate, reflectivity and mechanical properties of the mixture.

#### 4. Conclusions

Significant advances in thermal efficiency of transparent façades have been made in recent years particular through surface treatment technologies, such as high-performance films or active dyes. However, research in heat generation in exterior glazing derived from agricultural waste mixtures remains largely uncharted territory. In addition, while transparent substrates can be excellent for light conservation in buildings, often, there is need to control glare or increase privacy. Hence, research in new façade panels that can support energy generation and efficient reflectivity bear a strong potential for future building technologies.

The heating storage potential of the PMMA–sucrose mixture depends significantly in the concentration of sucrose. Our

simulation results indicate that the best condition to achieve optical and thermal advantages for heat storage and effective reflectivity in façade applications is ~0.5 of sucrose concentration. In this zone, the normalized heating rate is of a 20% reduction with a decrease in light absorption to 60% in comparison to 83% in pure PMMA. In parallel, if a higher need of reflectivity comparable or above existing IR thin film coatings or monolithic aerogel is required, a concentration range (60–75% sucrose) would be suitable. This would provide an advantageous normalized heating rate with almost a one third reduction in regards to pure PMMA. However, this range in principle presents more structural challenges. These simple simulation estimates present that the incorporation of sucrose into a PMMA substrate can potentially yield a substrate that operates as thermal mass and diffuses natural sunlight for combined energy savings and visual comfort.

When compared to alternative research of granular or particle-based infill for integrated thermal and optical performance of building enclosure panels our study provides a first indication of the advantages of agricultural waste in lieu of synthetic compounds for low cost and environmentally sensitive solutions. The knowledge provided by this study is valuable since it opens up new opportunities for incorporating agricultural waste in building composites that can act as thermal mass and have effective reflectivity with low material cost and low manufacturing energy. Projected estimates indicate that the use of the PMMA–sucrose mixture can provide cost-effective energy savings (thermal mass) and glare control for human comfort occupation. In combination, the mixture has the potential of significant low embodied energy decreasing the need for recycling pure PMMA, which up to date still presents multiple challenges.

The simulations presented in this paper enable a significant decrease in future physical testing of the PMMA–sucrose mixtures where additional parameters, such as fatigue and compressive strength, must be integrated for a comprehensive evaluation of construction suitability of the resulting material. The definition of a significantly smaller test is advantageous for time efficiency and decrease of unnecessary material waste. Future research will seek to: (i) test the fatigue behavior of PMMA–sucrose mixtures for a range of 40–60% concentration (sucrose); (ii) evaluate energy savings benefits for thermal mass and effective reflectivity of PMMA–sucrose mixtures for a range of 40–60% concentration for office buildings situated in cold and temperate climates in comparison to low-e and coated glazing panels; (iii) identify the structural potential of PMMA–sucrose in comparison to existing panels of recycled PMMA; (iv) identify the greatest potential for CO<sub>2</sub> savings over the life cycle of PMMA–sucrose in comparison to existing panels of recycled PMMA.

#### References

- [1] S. Jeska, *Transparent Plastics: Design and Technology*, Springer: Birkhäuser, Basel, Boston, 2008.
- [2] J. Knippers, J. Cremers, M. Gabler, J. Lienhard, *Construction Manual for Polymers + Membranes*, Birkhäuser Architecture, Basel, 2011.
- [3] A.W. LeCuyer, I. Liddell, S. Lehnert, B. Morris, *ETFE: Technology and Design*, Birkhäuser, Basel, Boston, 2008.
- [4] A. Watts, *Modern Construction Envelopes*, Springer, New York, 2011.
- [5] E. Dimitriadiou, A. Shea, *Experimental Assessment and Thermal Characterization of ETFE Foil*, 2012.
- [6] K.-H. Kim, A comparative life cycle assessment of a transparent composite façade system and a glass curtain wall system, *Energy and Buildings* 43 (12) (2011) 3436–3445.
- [7] A.K. Mohanty, M. Misra, L.T. Drzal, Sustainable bio-composites from renewable resources: opportunities and challenges in the green materials world, *Journal of Polymers and the Environment* 10 (1–2) (2002) 19–26.
- [8] T. Gengross, S. Slater, Biopolymers and the environment, *Science (New York, NY)* 299 (5608) (2003) 822.
- [9] J. Rybnicek, R. Lach, M. Lapcikova, J. Steidl, Z. Krulis, W. Grellmann, M. Slouf, Increasing recyclability of PC, ABS and PMMA: morphology and fracture behavior of binary and ternary blends, *Journal of Applied Polymer Science* 109 (5) (2008) 3210–3223.

- [10] D.S. Achilias, Chemical recycling of poly (methyl methacrylate) by pyrolysis. Potential use of the liquid fraction as a raw material for the reproduction of the polymer, *European Polymer Journal* 43 (6) (2007) 2564–2575.
- [11] C. Schittich, G. Staib, D. Balkow, M. Schuler, W. Sobek, *Glass Construction Manual (Construction Manuals)*, 2nd revised and expanded ed., Birkhäuser Architecture, Basel, 2007.
- [12] J.M.L. Reis, Fracture and flexural characterization of natural fiber-reinforced polymer concrete, *Construction and Building Materials* 20 (9) (2006) 673–678.
- [13] M.K. Yew, H.B. Mahmud, B.C. Ang, M.C. Yew, Effects of heat treatment on oil palm shell coarse aggregates for high strength lightweight concrete, *Materials & Design* 54 (2014) 702–707.
- [14] J. Khedari, P. Watsanasathaporn, J. Hirunlabh, Development of fibre-based soil-cement block with low thermal conductivity, *Cement and Concrete Composites* 27 (1) (2005) 111–116.
- [15] W. Yunus, A. bin, A. Rahman, Refractive index of solutions at high concentrations, *Applied Optics* 27 (16) (1988) 3341–3343.
- [16] W.T. Grondzik, A.G. Kwok, B. Stein, J.S. Reynolds, *Mechanical and Electrical Equipment for Buildings*, J. Wiley & Sons, New York, 2011.
- [17] P. Ihm, A. Nemri, M. Krarti, Estimation of lighting energy savings from daylighting, *Building and Environment* 44 (3) (2009) 509–514.
- [18] S. Kwon, I.-S. Koh, H.-W. Moon, J.-W. Lim, Y.J. Yoon, Model of inhomogeneous building facade for ray tracing method, *Electronics Letters* 44 (23) (2008) 1341–1342.
- [19] C.F. Reinhart, D.A. Weissman, The daylit area – correlating architectural student assessments with current and emerging daylight availability metrics, *Building and Environment* 50 (2012) 155–164.
- [20] C.G. Granqvist, Transparent conductors as solar energy materials: a panoramic review, *Solar Energy Materials and Solar Cells* 91 (17) (2007) 1529–1598.
- [21] K.A. Ismail, C.T. Salinas, J.R. Henriquez, Comparison between PCM filled glass windows and absorbing gas filled windows, *Energy and Buildings* 40 (5) (2008) 710–719.
- [22] S.N. Alamri, The temperature behavior of smart windows under direct solar radiation, *Solar Energy Materials and Solar Cells* 93 (9) (2009) 1657–1662.
- [23] J. Mohelníkova, Materials for reflective coatings of window glass applications, *Construction and Building Materials* 23 (5) (2009) 1993–1998.
- [24] M. Rubin, Calculating heat transfer through windows, *International Journal of Energy Research* 6 (4) (1982) 341–349.
- [25] D. Arasteh, M.S. Reilly, M.D. Rubin, A versatile procedure for calculating heat transfer through windows, Lawrence Berkeley Laboratory, 1989.
- [26] H. Manz, S. Brunner, L. Wullschleger, Triple vacuum glazing: heat transfer and basic mechanical design constraints, *Solar Energy* 80 (12) (2006) 1632–1642.
- [27] T.-P. Wang, L.-B. Wang, B.-Q. Li, A model of the long-wave radiation heat transfer through a glazing, *Energy and Buildings* 59 (Apr 2013) 50–61.
- [28] S.B. Sadineni, S. Madala, R.F. Boehm, Passive building energy savings: a review of building envelope components, *Renewable and Sustainable Energy Reviews* 15 (8) (2011) 3617–3631.
- [29] M.K. Urbikain, J.M. Sala, Analysis of different models to estimate energy savings related to windows in residential buildings, *Energy and Buildings* 41 (6) (2009) 687–695.
- [30] N. Eskin, H. Türkmen, Analysis of annual heating and cooling energy requirements for office buildings in different climates in Turkey, *Energy and Buildings* 40 (5) (2008) 763–773.
- [31] J.Y. Shin, G.Y. Yun, J.T. Kim, View types and luminance effects on discomfort glare assessment from windows, *Energy and Buildings* 46 (2012) 139–145.
- [32] S.N. Kasarova, N.G. Sultanova, C.D. Ivanov, I.D. Nikolov, Analysis of the dispersion of optical plastic materials, *Optical Materials* 29 (11) (2007) 1481–1490.
- [33] MicroChem Corp, *NANO<sup>TM</sup> PMMA and Copolymer Datasheet*, 2001.
- [34] M. Dowson, D. Harrison, S. Craig, Z. Gill, Improving the thermal performance of single-glazed windows using translucent granular aerogel, *International Journal of Sustainable Engineering* 4 (3) (2011) 266–280.
- [35] H. Gross, W. Singer, M. Totzeck, F. Blechinger, B. Achtner, *Handbook of Optical Systems*, vol. 2, Wiley Online Library, Weinheim, 2005.
- [36] C.F. Bohren, D.R. Huffman, *Absorption and Scattering of Light by Small Particles*, Wiley-VCH, Weinheim, 2008.
- [37] M. Born, E. Wolf, *Principles of Optics: Electromagnetic Theory of Propagation, Interference and Diffraction of Light*, Cambridge University Press Archive, Cambridge, New York, 1999.
- [38] W.C. Elmore, W.C. Elmore, M.A. Heald, *Physics of Waves*, Courier Dover Publications/McGraw-Hill, New York, 1969.
- [39] Z. Hashin, S. Shtrikman, A variational approach to the theory of the effective magnetic permeability of multiphase materials, *Journal of Applied Physics* 33 (10) (1962) 3125–3131.
- [40] E. Hecht, *Optics* 4th edition Optics 4th Edition by Eugene Hecht Reading, vol. 1, Addison-Wesley Publishing Company, MA, 2001.
- [41] J.D. Jackson, R.F. Fox, Classical electrodynamics, *American Journal of Physics* 67 (1999) 841.
- [42] O. Wiener, Zur Theorie der Refraktionskonstanten, in: Berichte über die Verhandlungen der Königlich-Sächsischen Gesellschaft der Wissenschaften zu Leipzig, vol. Math.-phys. Klasse, no. Band 62, 1910, pp. 256–277.
- [43] T.I. Zohdi, Computation of the coupled thermo-optical scattering properties of random particulate systems, *Computer Methods in Applied Mechanics and Engineering* 195 (41) (2006) 5813–5830.
- [44] T.I. Zohdi, On the optical thickness of disordered particulate media, *Mechanics of Materials* 38 (8) (2006) 969–981.
- [45] T.I. Zohdi, *Introduction to the Modelling and Simulation of Particulate Flows*, vol. 4, SIAM, Society for Industrial and Applied Mathematics, Philadelphia, PA, 2007.
- [46] S. Torquato, *Random Heterogeneous Materials: Microstructure and Macroscopic Properties*, Springer-Verlag, New York, 2002.
- [47] T.I. Zohdi, *Electromagnetic Properties of Multiphase Dielectrics: A Primer on Modeling, Theory and Computation*, vol. 64, Springer, Berlin, New York, 2012.
- [48] P.U. Jepsen, S.J. Clark, Precise ab-initio prediction of terahertz vibrational modes in crystalline systems, *Chemical Physics Letters* 442 (4) (2007) 275–280.
- [49] A. Tawansi, A. El-Khodary, H.M. Zidan, S.I. Badr, The effect of MnCl<sub>2</sub> filler on the optical window and the physical properties of PMMA films, *Polymer Testing* 21 (4) (2002) 381–387.
- [50] M.A. Darwish, Energy efficient air conditioning: case study for Kuwait, *Kuwait Journal of Science and Engineering* 32 (2) (2005) 209.
- [51] M.S. Alrubaih, M.F.M. Zain, M.A. Alghoul, N.L.N. Ibrahim, M.A. Shameri, O. Elayeb, Research and development on aspects of daylighting fundamentals, *Renewable and Sustainable Energy Reviews* 21 (2013) 494–505.
- [52] M.S. Rea, *The IESNA Lighting Handbook: Reference & Application*, Illuminating Engineering Society of North America, New York, NY, 2000.
- [53] C. Buratti, E. Moretti, Glazing systems with silica aerogel for energy savings in buildings, *Applied Energy* 98 (2012) 396–403.